Laboratory Investigation
https://doi.org/10.1038/s41374-019-0354-2

ARTICLE

Development of multiple features of antigen-induced asthma pathology in a new strain of mast cell deficient BALB/c-*Kit*$^{W\text{-}sh/W\text{-}sh}$ mice

Joseph D. Hernandez[1,2] · Mang Yu[1] · Riccardo Sibilano[1] · Mindy Tsai[1] · Stephen J. Galli[1,3]

Received: 12 August 2019 / Revised: 25 October 2019 / Accepted: 29 October 2019
© The Author(s), under exclusive licence to United States and Canadian Academy of Pathology 2019

Abstract

Mast cell-deficient mice are widely used to identify and quantify contributions of mast cells to diverse biological responses in vivo, including allergic inflammation. However, despite the fact that scores of genes have been identified as modifiers of allergic inflammation, most mast cell-deficient models have been available only on a single genetic background. We transferred the *Kit*$^{W\text{-}sh}$ allele onto the BALB/c background to generate BALB/c mast cell-deficient mice (BALB/c-*Kit*$^{W\text{-}sh/W\text{-}sh}$). BALB/c-*Kit*$^{W\text{-}sh/W\text{-}sh}$ mice have dramatically reduced mast cell numbers (0–2% of wild type) in all tissues examined, as well as subtle hematologic differences from the corresponding wild type mice, including splenomegaly with evidence of increased splenic hematopoiesis. We examined in BALB/c-*Kit*$^{W\text{-}sh/W\text{-}sh}$ mice models of allergic inflammation that are substantially diminished in C57BL/6-*Kit*$^{W\text{-}sh/W\text{-}sh}$ mast cell-deficient mice. In a model of acute allergic inflammation, i.e., IgE-dependent passive cutaneous anaphylaxis, both ear swelling and leukocyte infiltration were largely or entirely absent in BALB/c-*Kit*$^{W\text{-}sh/W\text{-}sh}$ mice. In contrast, in two different models of allergic airway inflammation, airway hyperresponsiveness, lung inflammation, and airway remodeling developed robustly in mast cell-deficient BALB/c-*Kit*$^{W\text{-}sh/W\text{-}sh}$ mice. These results support the conclusion that the importance of mast cell contributions in various models of allergic inflammation may be at least partially determined by genetic background.

Introduction

Mast cell- (MC-) deficient mouse models have been used to identify and quantify roles for MCs in host defense against infections and venoms, in inflammatory disorders, and in models of atopic diseases. Two approaches have been employed to generate MC-deficient mice; initially described models have defects in c-*kit* expression or function that result in profound MC deficiency, whereas more recently described models utilize multiple genetic approaches that result in MC-deficiency independently of effects on c-*kit* (reviewed [1–3]). However, until recently, most of these approaches have only been available on a single genetic background, limiting the ability to evaluate potential effects of genetic background on roles for MCs in individual biological responses in vivo.

Predominantly two types of c-*kit* mutant MC-deficient mice have been used to investigate the function of MCs in vivo, WBB6F$_1$-*Kit*$^{W/W\text{-}v}$ and C57BL/6-*Kit*$^{W\text{-}sh/W\text{-}sh}$ mice [2, 4–8]. *Kit*$^{W/W\text{-}v}$ mice are profoundly MC deficient [5], but also have numerous other phenotypic abnormalities as a result of decreased c-*kit* expression, including a melanocyte deficiency, sterility, macrocytic anemia, neutropenia, basopenia, decreased numbers of intestinal intraepithelial lymphocytes, and the development in adulthood of spontaneous dermatitis, gastric ulcers, and squamous papillomas of the forestomach [2, 7, 9–15]. The *Kit*$^{W\text{-}sh/W\text{-}sh}$ mouse has a 3 cM inversion ~72 kb upstream of the c-*kit* transcriptional start site [16], resulting in severely impaired c-*kit* expression and

Supplementary information The online version of this article (https://doi.org/10.1038/s41374-019-0354-2) contains supplementary material, which is available to authorized users.

✉ Stephen J. Galli
sgalli@stanford.edu

[1] Department of Pathology and the Sean N. Parker Center for Allergy & Asthma Research, Stanford University School of Medicine, Stanford, CA, USA

[2] Department of Pediatrics, Division of Immunology, Allergy and Rheumatology, Stanford University School of Medicine, Stanford, CA, USA

[3] Department of Microbiology and Immunology, Stanford University School of Medicine, Stanford, CA, USA

Published online: 19 December 2019

MC deficiency [4, 17, 18], as well additional phenotypic abnormalities that are not fully overlapping with those of WBB6F$_1$-*Kit*$^{W/W-v}$ mice. Like WBB6F$_1$-*Kit*$^{W/W-v}$ mice, C57BL/6-*Kit*$^{W-sh/W-sh}$ mice are deficient in melanocytes but are fertile, are not anemic, and have increased numbers of neutrophils and basophils, increased splenic hematopoiesis, and normal numbers of intraepithelial lymphocytes, and they do not exhibit a high incidence of spontaneous dermatitis, gastric ulcers, or papillomas [4, 13, 16, 19].

Multiple observations indicate that genetic background can make important contributions to the development of Th2 immunity and atopic disease. First, many genes have been shown to contribute to the development of atopic disease in humans, with over 100 genes identified as modifiers to asthma susceptibility alone [20–22]. Second, it has long been appreciated that some strains of mice, particularly BALB/c mice, have an intrinsic bias toward developing type 2 immune responses [23]. Until recently, no MC-deficient models have been available on the BALB/c background, and perhaps more importantly, few MC-deficient models have been available on multiple genetic backgrounds [24, 25], thereby permitting the evaluation of which aspects of the model may be influenced by genetic background.

Recently two studies have identified roles for MCs in disease models that may be heavily influenced by the genetic background of the mice. In a model of parasite infection using c-*kit*-independent MC-deficient mice, MCs contributed to the expulsion of *Stongyloides ratti* in Treg-depleted BALB/c mice, but not in Treg-depleted C57BL/6 mice [25]. In a model of ovalbumin-induced allergic airway inflammation, *Kit*$^{W-sh/W-sh}$ mice on the BALB/c background developed airway inflammation and airway hyperreactivity equivalent to that observed in the corresponding *Kit*$^{+/+}$ *mice* [24]. By contrast, *Kit*$^{W-sh/W-sh}$ mice on the C57BL/6 background developed diminished airway inflammation and airway hyperreactivity compared with that in their *Kit*$^{+/+}$ counterparts [24], in confirmation of prior studies with such mice that employed a different model of ovalbumin-induced allergic airway inflammation [26, 27].

In the present study, we report using the agouti-colored BALB/c strain, C.B6-*Tyr*$^{+}$ *Hbb*^{s}*/J*, to create a new strain of BALB/c MC-deficient mice by transferring the *Kit*$^{W-sh}$ allele onto the normally albino BALB/c background in a manner that maintains the ease of visual genotyping; such mice hereafter are referred to as BALB/c-*Kit*$^{W-sh/W-sh}$ mice. We confirmed that BALB/c-*Kit*$^{W-sh/W-sh}$ mice are profoundly MC-deficient and characterized the hematologic profiles of such BALB/c-*Kit*$^{W-sh/W-sh}$ mice. Finally, we examined how genetic background can affect the phenotype of the pathology elicited in three models of allergic inflammation: IgE-dependent passive cutaneous anaphylaxis and two models of antigen-induced chronic allergic inflammation of the airways [27].

Materials and methods

Animals

C57BL/6J-*Kit*$^{W-sh/+}$ mice (B6.Cg-*Kit*$^{W-sh}$/HNihrJaeBsmGlliJ, Jackson Laboratory, Sacramento, California, USA), were previously generated in our lab by backcrossing *Kit*$^{W-sh/+}$ mice (a generous gift of Peter Besmer, Memorial Sloan-Kettering Cancer Center) for more than 11 generations to C57BL/6J mice (Jackson Laboratory) [13]. C57BL/6J-*Kit*$^{W-sh/+}$ mice were backcrossed for 11 generations or more to C.B6-*Tyr*$^{+}$ *Hbb*^{s}*/J* (Jackson Laboratory), an agouti-colored mouse that had previously been backcrossed to BALB/c for more than 11 generations. The resulting C.B6- *Kit*$^{W-sh}$ *Tyr*$^{+}$ *Hbb*^{s}*/J* are herein referred to as BALB/c-*Kit*$^{W-sh/W-sh}$ mice. All animal husbandry and experiments were performed in accordance with the 'Guide for the Care and Use of Laboratory Animals' published by the National Academy Press (revised, 1996), and with approval of the Stanford University Institutional Animal Care and Use Committee.

Cell quantification and flow cytometry

Red blood cell indices were measured by an automated hematology analyzer. Leukocyte populations in blood were assessed by flow cytometry as follows: neutrophils Gr-1^{+}, T cells CD3^{+}, B cells B220^{+}, monocytes F4/80^{+} Gr-1^{-}, eosinophils CCR3^{+} SSC^{hi}, basophils FcεRIα^{+} CD49b^{+}. Peritoneal cells were isolated by peritoneal lavage with PBS. MCs were identified by staining peritoneal cells for FcεRIα and CD117 (c-kit). RBCs were lysed in ACK buffer (0.15 M NH_4Cl, 1 mM $KHCO_3$, 0.1 mM EDTA). Cells were blocked with anti-CD16/32 for 10 min on ice, before staining with antibodies for flow cytometry for 30 min on ice. Propidium iodide (BD Biosciences, San Jose, California, USA) was used to exclude dead cells from analysis. Antibodies used were: FcεRIα (MAR-1; eBiosciences, San Diego, California, USA), CD117 (2B8; BD Biosciences), CD49b (DX5; Biolegend, San Diego, California, USA), CCR3 (TG14; Biolegend), B220 (RA3-6B2, BD Biosciences), CD3ε (145-2C11; eBiosciences), Gr-1 (RB6-8C5; eBiosciences), F4/80 (BM8; eBiosciences), CD16/32 (2.4G2, Bio X Cell, West Lebanon, New Hampshire, USA).

IgE-dependent passive cutaneous anaphylaxis

Ear pinnae of mice were injected intradermally with 20 ng of IgE anti-DNP (clone ε26 [28], kindly provided by Fu-Tong Liu, University of California Davis) in HMEM-Pipes buffer or with HMEM-Pipes buffer as a vehicle control. The experimentor was blinded to the identity of ear pinnae containing antibody vs. vehicle. The following day the mice

were challenged i.v. with 100 µg $DNP_{30–40}$-conjugated to human serum albumin (DNP-HSA; Sigma-Aldrich) in 0.9% NaCl. Ear thickness was measured with a dial thickness gauge (G-1A; Ozaki, Tokyo, Japan) immediately before and at indicated intervals following challenge. Injections and measurements were done under isoflurane anesthesia. Six hours following challenge, mice were sacrificed and the ear pinnae were collected for histology.

Induction of antigen-dependent chronic inflammation of the airways

Allergic airway inflammation to OVA was induced using a protocol similar to that previously described [27]. Briefly, mice were immunized with 50 µg OVA (Sigma-Aldrich, St. Louis, Missouri, USA) i.p. in 0.1 ml PBS on days 1, 4, and 7. Starting on day 12, mice were challenged i.n. with 20 µg OVA in 30 µl PBS weekly for a total of 8 weeks. Control mice received PBS alone for i.p. injections and i.n. challenges. Airway responses to OVA or PBS were assessed at indicated times following challenge using whole body plethysmography (BUXCO system, St. Paul, Minnesota, USA) to measure Penh for 5 min. Mice were sacrificed by CO_2 inhalation 24 h following final antigen challenge. The left lung was ligated, removed, and flash frozen. The right lung was lavaged with Hanks' balanced salt solution, before instilling 10% formalin for fixation prior to histology. Bronchoalveolar lavage (BAL) cells were counted in a hematocytometer. Differential leukocyte counts were performed visually in HEMA-3-stained cytospin preparations.

Allergic inflammation to house dust mite antigen (HDM) *D. pteronissynus* was induced as previously described [29]. Briefly, mice were sensitized with 100 µg of HDM (Greer, Lenoir, NC, USA) in 30 µl of PBS i.n. on days 1, 3, and 5; mice were then challenged with 20 µg of HDM in 30 µl of PBS on days 13, 18, 23, 28, 33, 38, 43, 48, 52, and 57. Control mice received PBS for i.n. sensitization and challenge. Whole body plethysmography was performed at various time points over 24 h following final challenge as per above. One day after the final HDM or PBS i.n. challenge, invasive measurements of airway resistance (R_L; Buxco systems) were performed in anesthetized, tracheostomized, and mechanically-ventilated mice. Increasing concentrations (0, 2.5, 5, 7.5, and 10 mg/ml) of aerosolized methacholine (Sigma-Aldrich) were administered followed by measurements of airway resistance for 3 min after each dose. Mice were immediately sacrificed, BAL fluid was recovered, and the lungs prepared for histology as described above.

Histology

Tissues were fixed in 10% neutral buffered formalin prior to embedding in paraffin and sectioning. Sections were stained with Toluidine blue to perform MC counts in various tissues, with H&E to examine inflammation and count numbers of infiltrating leukocytes, and PAS to count goblet cells. Ten or more low (10× objective) powered fields (for MC and megakaryocyte counts), medium (20× objective) powered fields (for goblet cell counts), or high (40× objective) powered fields (for infiltrating leukocytes) were examined for each mouse. All of the counts were done on blinded slides. Cell counts were determined per unit area of tissue for MC numbers and infiltrating leukocytes, or per length of basement membrane for goblet cells.

Statistical analysis

Statistical analysis was done using Graph Pad Prism (La Jolla, California, USA). Comparison of two groups was done using a *t* test. Comparison of two or more groups was done using multiple *t* tests with Holm-Sidak correction for multiple *t* tests, ANOVA or 2-way ANOVA as appropriate, and indicated in figure legends. In all cases an alpha of 0.05 was considered significant.

ELISA

Cytokine, chemokine, and antibody concentrations were measured via ELISA. Plasma collected at the time of sacrifice was assayed for OVA-specific IgE and IgG_1 similarly to previously described [30]. Briefly, plates were coated with 100 µg/ml OVA, and blocked with 1% BSA, prior to incubation with diluted plasma. Bound antibody was detected with biotinylated rat anti-IgG_1 (clone A85-1, BD Pharmigen) or rat anti-IgE (clone R35-118, BD Pharmigen), followed by addition of streptavidin-HRP (BD Pharmigen) and supersensitive TMB (Sigma-Aldrich) as a substrate. Lung homogentates were prepared from half of the left lung as previously described [27] in T-PER buffer (ThermoFisher Scientific, Waltham, MA, USA). ELISAs for IL-5 (eBioscience), eotaxin (R&D Systems, Minneapolis, MN, USA), and RANTES (R&D Systems) were performed according to the manufacturers' instructions.

Results

BALB/c-*Kit*$^{W\text{-}sh/W\text{-}sh}$ mice are profoundly deficient in mast cells

Backcrossing of the *Kit*$^{W\text{-}sh}$ allele onto an agouti brown strain of BALB/c mice (Fig. 1a) enabled easy genotyping by coat pigmentation. BALB/c-*Kit*$^{W\text{-}sh/W\text{-}sh}$ mice lacked most skin and fur pigmentation, and BALB/c-*Kit*$^{+/W\text{-}sh}$ mice displayed a characteristic "sash" pigmentation pattern. In heterozygote breeding, pups were weaned with the expected

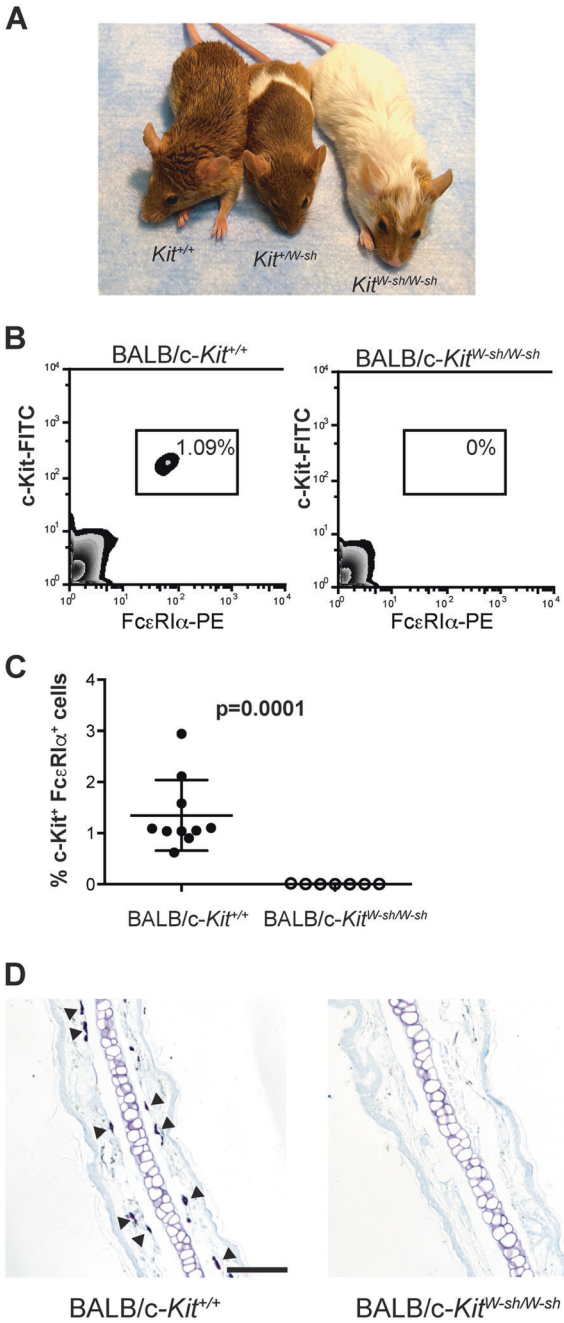

Fig. 1 BALB/c-*Kit*$^{W\text{-}sh/W\text{-}sh}$ mice are mast cell-deficient. a BALB/c-*Kit*$^{W\text{-}sh/W\text{-}sh}$ mice display a marked dilution of the agouti coat color of the wild type mice, while BALB/c-*Kit*$^{+/W\text{-}sh}$ mice display a dilution of the coat color in the characteristic "sash" pattern. Cells from peritoneal lavage were analyzed by flow cytometry for expression of the mast cell markers c-Kit and FcεRIα (**b**), and mast cells were quantified as a percentage of the total live peritoneal cells (**c**). Tissues, including ear pinnae (**d**), were examined for mast cells by staining with Toluidine blue. Some of the many mast cells present in the section of a wild type BALB/c-*Kit*$^{+/+}$ mouse are indicated by solid arrowheads, whereas no mast cells are seen in this section of ear pinna from a BALB/c-*Kit*$^{W\text{-}sh/W\text{-}sh}$ mice. $n = 7$–10 mice per group for peritoneal cell analysis (**c**), combined from 2 independent experiments. Lines in **c** represent mean value ± s.e.m. Scale bars in **d** indicate 100 µm.

Table 1 Mast cell numbers in tissues.

Tissue	BALB/c-*Kit*$^{+/+}$	BALB/c- *Kit*$^{W\text{-}sh/W\text{-}sh}$ (% *Kit*$^{+/+}$ value)	*p* value
Trachea	15.9 ± 4.4	0.09 ± 0.06 (0.6)	<0.01
Lung	0.8 ± 0.3	0.02 ± 0.01 (2.5)	<0.02
Dorsal skin	14.2 ± 2.7	0	<0.01
Ear pinnae	80.1 ± 6.0	0.22 ± 0.12 (0.3)	<0.01
Forestomach	44.3 ± 4.9	0	<0.01
Glandular stomach	13.9 ± 2.2	0	<0.01
Duodenum	8.2 ± 2.2	0	<0.01
Spleen	1.3 ± 0.3	0	<0.01

Values are expressed as means (cells/mm^2) ± s.e.m. *p* values determined by two-tailed *t* test (unpaired)

Kit$^{+/+}$ $n = 10$, *Kit*$^{W\text{-}sh/W\text{-}sh}$ $n = 8$, except ear pinnae: *Kit*$^{+/+}$ $n = 6$, *Kit*$^{W\text{-}sh/W\text{-}sh}$ $n = 7$

ratio of genotypes, but overall exhibited a higher mortality rate than that reported for the parental BALB/c strain, 28% vs. 7.4% respectively [31].

Adult BALB/c-*Kit*$^{W\text{-}sh/W\text{-}sh}$ mice lacked detectable numbers of MCs in the peritoneal cavity (Fig. 1b, c) and many other tissues (Fig. 1d; Table 1). However, small numbers of MCs were detected in some of the tissues examined (Table 1), with reductions in MC numbers relative to those in the corresponding BALB/c-*Kit*$^{+/+}$ mice in the lung, trachea, and ear pinnae by 40 fold, 176 fold, and 360 fold, respectively.

BALB/c-*Kit*$^{W\text{-}sh/W\text{-}sh}$ mice exhibit splenomegaly with hematologic anomalies

Because *Kit* mutations have been associated with multiple hematologic abnormalities [2, 4, 13, 16, 19], we examined the red blood cell and leukocyte profiles of BALB/c-*Kit*$^{W\text{-}sh/W\text{-}sh}$ mice. Red blood cells from BALB/c-*Kit*$^{W\text{-}sh/W\text{-}sh}$ have slightly increased mean corpuscular volume and slightly decreased hemoglobin levels (Fig. 2a). While there was a trend toward decreased hematocrit levels in mutant mice, these differences were not statistically significant for the numbers of mice analyzed. We observed increased numbers of T cells in blood from BALB/c-*Kit*$^{W\text{-}sh/W\text{-}sh}$ mice compared with control BALB/c-*Kit*$^{+/+}$ mice (Fig. 2b). Numbers of other leukocyte cell populations were quite variable between individual mice of the same genotype, and therefore the differences in these between the BALB/c-*Kit*$^{W\text{-}sh/W\text{-}sh}$ and corresponding wild type mice were not statistically significant. Notably, among these statistically insignificant trends, we observed increased numbers of blood neutrophils and basophils, a finding also observed in C57BL/6-*Kit*$^{W\text{-}sh/W\text{-}sh}$ mice [13, 16, 19].

Splenomegaly was apparent on necropsy of some BALB/c-*Kit*$^{W\text{-}sh/W\text{-}sh}$ mice, and spleen weights confirmed the

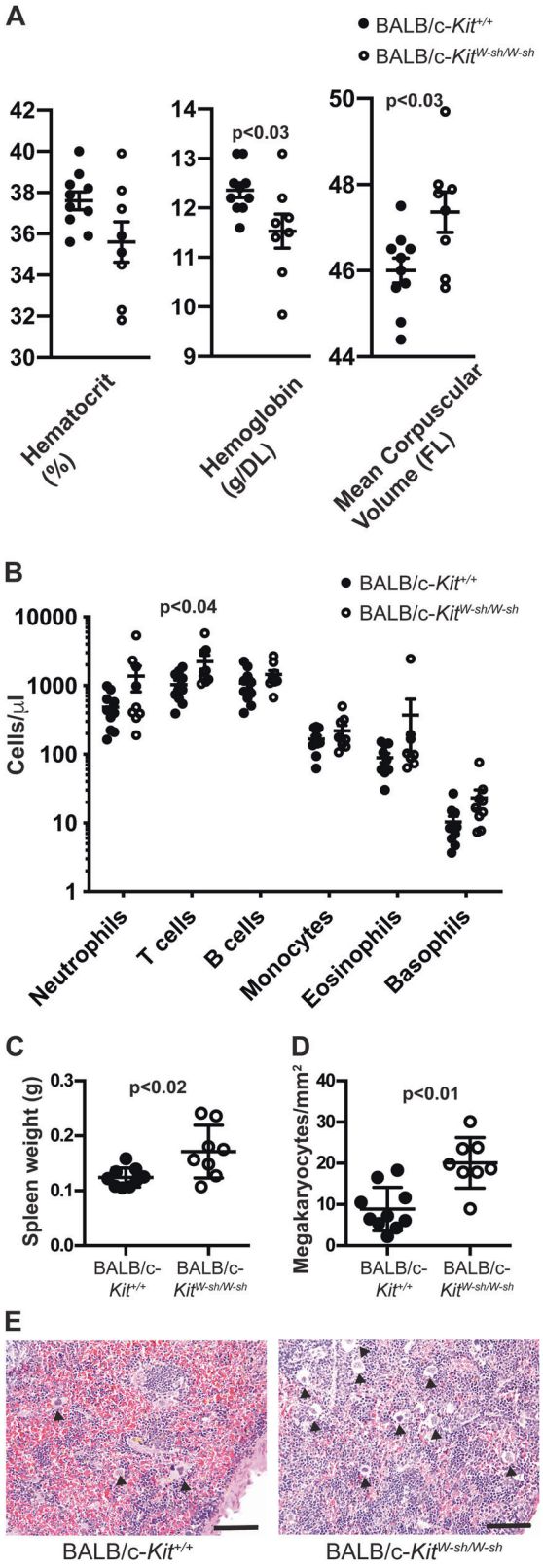

Fig. 2 BALB/c-*Kit*$^{W\text{-}sh/W\text{-}sh}$ mice have enlarged spleens and minor hematologic abnormalities. a Red blood cell indices in peripheral blood samples were measured by automated analysis. **b** Differential cell counts were determined by flow cytometry for neutrophils (GR1$^+$), T cells (CD3$^+$), B cells (B220$^+$), monocytes (F4/80$^+$), eosinophils (CCR3$^+$) and basophils (CD49b$^+$FcεRIα$^+$). **c** Spleen weights. **d** Megakaryocyte counts from spleen sections. **e** Sections of spleen showing increased hematopoiesis and numerous megakaryocytes (solid arrowheads) in spleen section from the BALB/c-*Kit*$^{W\text{-}sh/W\text{-}sh}$ mouse. **a**–**d** $n = 7$–10 mice per group, combined from two independent experiments. Lines represent mean values ± s.e.m. Scale bars in **e** indicate 100 µm.

presence of splenomegaly in such mice (Fig. 2c). Even among age-matched mice, the degree of splenomegaly displayed considerable variability. Splenomegaly may be partially explained by increased splenic hematopoiesis in BALB/c-*Kit*$^{W\text{-}sh/W\text{-}sh}$ mice (Fig. 2e) as evidenced by increased megakaryocyte numbers in the spleen (Fig. 2d). Variable splenomegaly and increased splenic hematopoiesis were also seen in C57BL/6-*Kit*$^{W\text{-}sh/W\text{-}sh}$ mice [16].

IgE-dependent PCA is absent in BALB/c-*Kit*$^{W\text{-}sh/W\text{-}sh}$ mice

To determine if diminished MC numbers in BALB/c-*Kit*$^{W\text{-}sh/W\text{-}sh}$ mice resulted in reduced MC function in vivo, we assessed IgE-dependent PCA, an IgE and MC-dependent response [32]. BALB/c-*Kit*$^{+/+}$ mice developed significant ear pinnae swelling that peaked at ~30 min following antigen challenge (Fig. 3a). In contrast, BALB/c-*Kit*$^{W\text{-}sh/W\text{-}sh}$ mice developed ear swelling following antigen challenge that was not appreciably different than that in the control ear pinnae which had been injected with vehicle (Fig. 3a). Many leukocytes infiltrated IgE-treated ears in BALB/c-*Kit*$^{+/+}$ ear pinnae, whereas few leukocytes infiltrated IgE-treated ear pinnae in BALB/c-*Kit*$^{W\text{-}sh/W\text{-}sh}$ mice (Fig. 3b, c). These observations indicate that insufficient numbers of MCs exist in ear skin in BALB/c-*Kit*$^{W\text{-}sh/W\text{-}sh}$ mice to mediate early or late phase IgE- and MC-dependent inflammation at that site under the conditions tested.

Chronic allergic inflammation of the airways can develop in BALB/c-*Kit*$^{W\text{-}sh/W\text{-}sh}$ mice

We also assessed the extent to which BALB/c-*Kit*$^{W\text{-}sh/W\text{-}sh}$ vs. the corresponding *Kit*$^{+/+}$ mice could develop various features of allergic airway inflammation, using two models of chronic allergic inflammation of the airways in which the development of these features were substantially enhanced by MCs in C57BL/6 mice [27].

In contrast to our previous observations in C57BL/6 mice [27], specifically, that many features of a well-characterized model of OVA-induced airway inflammation require MCs for optimal development, many features of OVA-induced airway inflammation in BALB/c-*Kit*$^{W\text{-}sh/W\text{-}sh}$ mice were MC-independent (Fig. 4a–g) under the

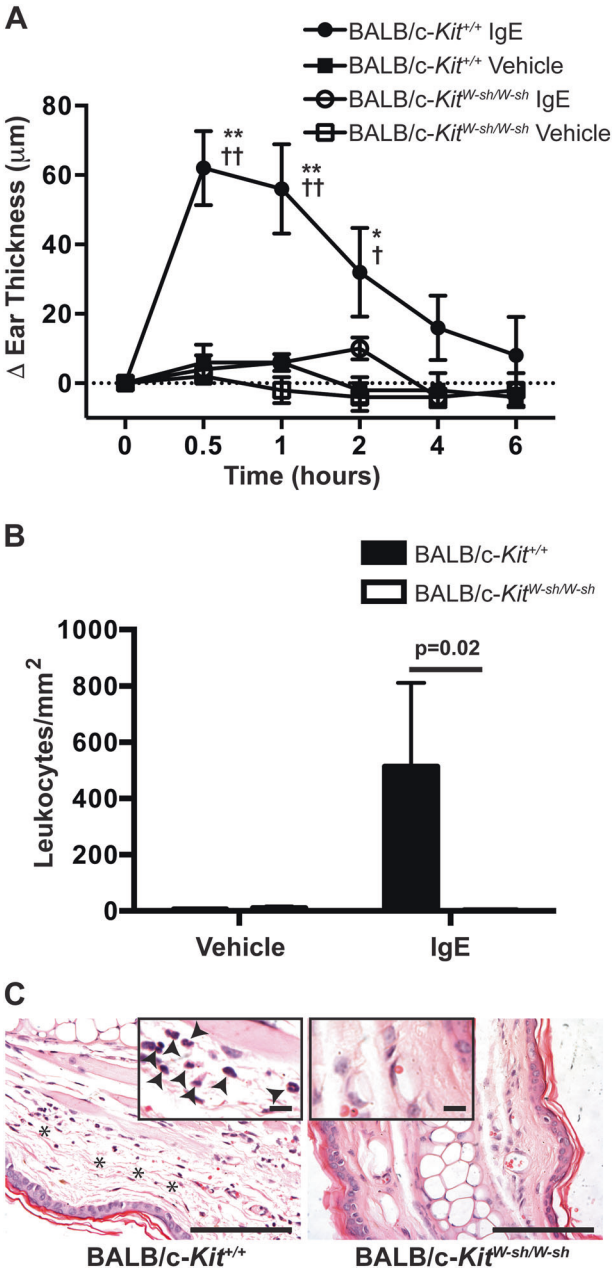

Fig. 3 IgE-dependent passive cutaneous anaphylaxis is diminished in BALB/c-*Kit*$^{W\text{-}sh/W\text{-}sh}$ mice. Mice were injected i.d. with vehicle (saline) in one ear and anti-DNP-IgE in the opposite ear. 24 h later, mice were challenged i.v. with DNP-HSA. **a** Ear swelling was measured at the time intervals indicated. Mice were killed 6 h after injection of DNP-HSA and leukocytes present in the dermis were counted (**b**) in hematoxylin & eosin (H&E)-stained sections of ear pinnae at the sites which had been injected with saline or anti-DNP-IgE (**c**). **c** Histology of the site which had been injected with anti-DNP-IgE shows edema (indicated with asterisks) and the presence of leukocytes in the dermis (solid arrowheads in the inset) in sections from wild type BALB/c-*Kit*$^{+/+}$ mice but not in those of BALB/c-*Kit*$^{W\text{-}sh/W\text{-}sh}$ mice. $n = 5$ mice per group. Mean values are shown ± s.e.m. for one of two independent experiments, each of which gave similar results. $^{**}p < 0.0001$ and $^{*}p < 0.001$ for BALB/c-*Kit*$^{+/+}$ IgE vs. BALB/c-*Kit*$^{+/+}$ vehicle; $^{\dagger\dagger}p < 0.0001$ and $^{\dagger}p < 0.05$ for BALB/c-*Kit*$^{+/+}$ IgE vs. BALB/c-*Kit*$^{W\text{-}sh/W\text{-}sh}$ IgE as determined by 2-way ANOVA. Scale bars in **c** indicate 100 μm and, for the insets, 13 μm.

conditions tested. Three hours following intranasal challenge with OVA, both BALB/c-*Kit*$^{+/+}$ and BALB/c-*Kit*$^{W\text{-}sh/W\text{-}sh}$ mice exhibited an increased Penh, as assessed by whole body plethysmography (Fig. 4a). One day following antigen challenge, BAL fluids demonstrated similarly increased numbers of inflammatory cells in both BALB/c-*Kit*$^{+/+}$ and BALB/c-*Kit*$^{W\text{-}sh/W\text{-}sh}$ antigen-treated mice compared with values in those mice which had been challenged with buffer alone (Fig. 4b). Although we observed somewhat increased eosinophil numbers in the BAL fluid from BALB/c-*Kit*$^{W\text{-}sh/W\text{-}sh}$ mice, this was not statistically significant (Fig. 4b) nor was it observed in a second experiment performed with older mice (56,400 ± 22,200 eosinophils in four BALB/c-*Kit*$^{+/+}$ mice vs. 38,000 ± 14,000 eosinophils in five BALB/c-*Kit*$^{W\text{-}sh/W\text{-}sh}$ mice). Moreover, except for eotaxin, which in OVA-sensitized mice was higher in BALB/c-*Kit*$^{+/+}$ mice than in BALB/c-*Kit*$^{W\text{-}sh/W\text{-}sh}$ mice, IL-5 and RANTES concentrations were not higher in OVA-sensitized BALB/c-*Kit*$^{W\text{-}sh/W\text{-}sh}$ mice compared with OVA-sensitized BALB/c-*Kit*$^{+/+}$ mice (Supplementary Fig. 1).

On histology, we observed comparable perivascular and peribronchiolar infiltrates of leukocytes in BALB/c-*Kit*$^{+/+}$ and BALB/c-*Kit*$^{W\text{-}sh/W\text{-}sh}$ mice (Fig. 4c, d). As a measure of airway remodeling, numbers of airway goblet cells (Fig. 4e, f) were also similar between wild type and BALB/c-*Kit*$^{W\text{-}sh/W\text{-}sh}$ mice. Finally, a MC deficiency did not appear to influence blood levels of OVA-specific IgE and IgG_1, as we observed no differences in OVA-specific IgE or IgG_1 titers between BALB/c-*Kit*$^{+/+}$ and BALB/c-*Kit*$^{W\text{-}sh/W\text{-}sh}$ mice (Fig. 4g). Previously, we did not observe differences in OVA-specific antibody titers in this model between C57BL/6-*Kit*$^{+/+}$ and C57BL/6-*Kit*$^{W\text{-}sh/W\text{-}sh}$ mice either [27].

To test whether genetic background would similarly affect the airway inflammation induced by a different antigen, we utilized a second model of allergic airway inflammation using HDM [29], an antigen which induces sensitization for airway inflammation and airway hyperreactivity in many human asthma patients [33, 34]. In C57BL/6 mice, this model results in the development of airway hypersensitivity to methacholine (as assessed by invasive measurements of lung resistance [R_L]) and airway inflammation that are significantly diminished in MC-deficient C57BL/6-*Kit*$^{W\text{-}sh/W\text{-}sh}$ mice (Supplementary Fig. 2). Specifically, C57BL/6-*Kit*$^{W\text{-}sh/W\text{-}sh}$ mice exhibited markedly reduced airway hyperresponsiveness to methacholine (Supplementary Fig. 2A), reduced numbers of inflammatory cells in the BAL fluid (Supplementary Fig. 2B), and decreased histologic evidence of inflammation (Supplementary Fig. 2C, D) when compared with the corresponding wild type mice. However, numbers of goblet cells in HDM-treated C57BL/6-*Kit*$^{W\text{-}sh/W\text{-}sh}$ mice were similar to those in wild type mice (Supplementary Fig. 2E, F).

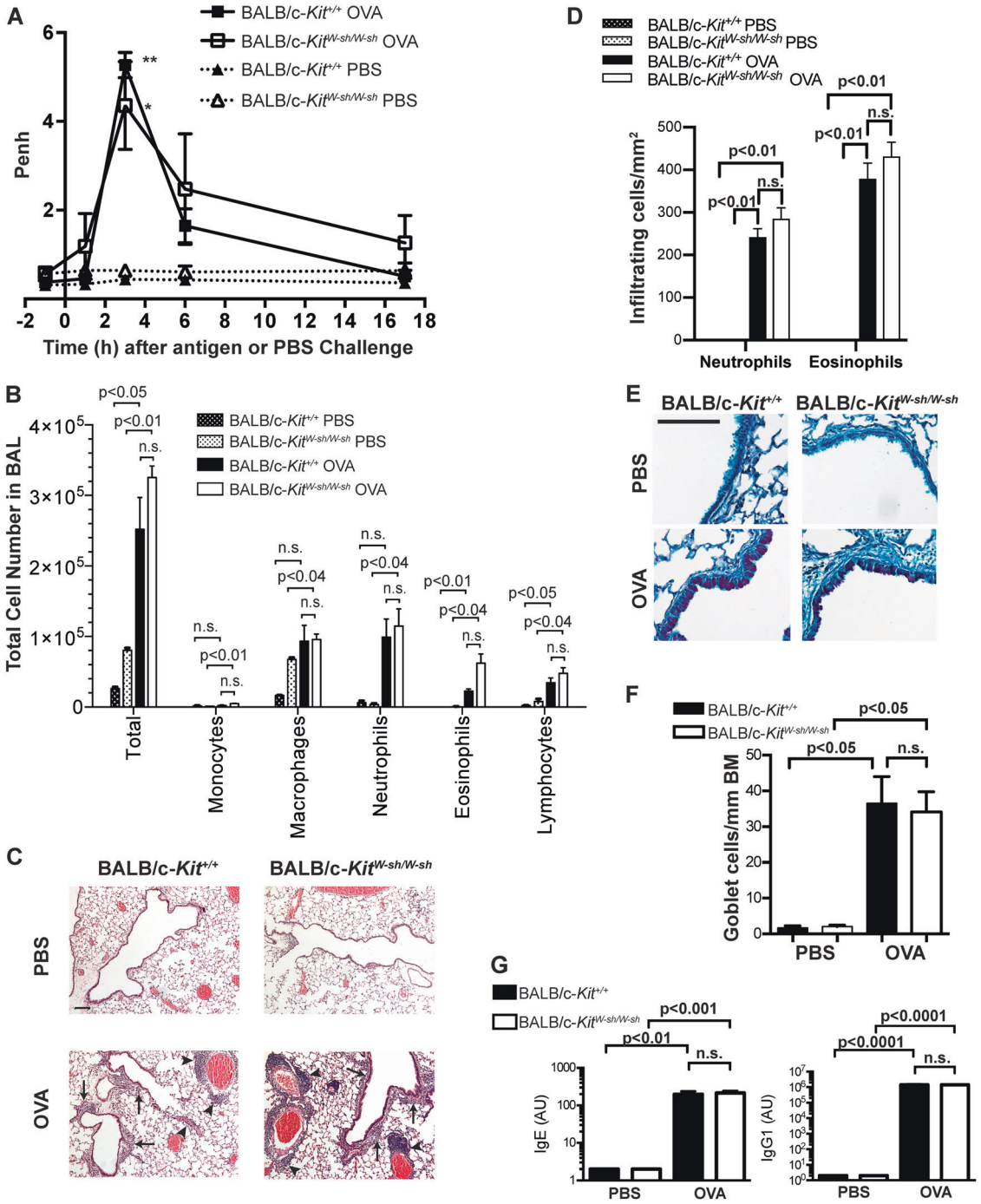

In contrast to results in the C57BL/6-*Kit*$^{W\text{-}sh/W\text{-}sh}$ mice, BALB/c-*Kit*$^{W\text{-}sh/W\text{-}sh}$ mice developed similar levels of airway hyperresponsiveness, as assessed by invasive measurements of lung resistance (R_L) (Fig. 5a), similar numbers of inflammatory cells in the BAL fluid (Fig. 5b), and similar histologic evidence of inflammation (Fig. 5c, d), as well as similar number of goblet cells (Fig. 5e, f), when compared with the corresponding wild type BALB/c-*Kit*$^{+/+}$ mice. In this HDM model, neither C57BL/6 nor BALB/c wild type (nor the corresponding MC-deficient mice) exhibited increased Penh following antigen challenge (data not shown).

Taken together, these data indicate that many features of two models of chronic allergic inflammation of the airways that are substantially diminished in MC-deficient C57BL/6-*Kit*$^{W\text{-}sh/W\text{-}sh}$ mice [27] can be expressed at wild type levels in MC-deficient BALB/c-*Kit*$^{W\text{-}sh/W\text{-}sh}$ mice.

◀ **Fig. 4 Airway hyperresponsiveness to antigen, lung inflammation, and airway remodeling develop in an OVA-induced model of chronic asthma elicited in BALB/c-*Kit*$^{W\text{-}sh/W\text{-}sh}$ mice. a** Penh values were measured 1 h before and 1, 3, 6, and 17 h after the eighth PBS or OVA challenge. **b** Leukocyte numbers in bronchoalveolar lavage fluid (BALF) were determined by manual counting and by differential counts on cytospin slides. **c** Histology in H&E-stained sections of lungs. Solid arrowheads indicate perivascular inflammation, and solid arrows indicate peribronchiolar inflammation. **d** Numbers of infiltrating leukocytes quantified per mm^2 of airway. **e** PAS stain of mouse airways. Scale bars in **c** and **e** indicate 100 µm. **f** Goblet cell numbers per mm of airway basement membrane (BM). **g** Plasma titers of OVA-specific IgE and IgG$_1$ as determined by ELISA. Results are expressed as arbitrary units. For Penh measurements and BAL cell counts, for OVA-sensitized and challenged mice (OVA mice), $n = 9$ for BALB/c-*Kit*$^{W\text{-}sh/W\text{-}sh}$ and $n = 5$ for BALB/c-*Kit*$^{+/+}$ mice; for PBS mock-sensitized and challenged mice (PBS mice), $n = 4$ for BALB/c-*Kit*$^{W\text{-}sh/W\text{-}sh}$ and $n = 3$ for BALB/c-*Kit*$^{+/+}$ mice. For goblet cell counts, $n = 5$ for BALB/c-*Kit*$^{W\text{-}sh/W\text{-}sh}$ OVA and $n = 4$ for BALB/c-*Kit*$^{+/+}$ OVA mice, and $n = 4$ for BALB/c-*Kit*$^{W\text{-}sh/W\text{-}sh}$ PBS and $n = 3$ for BALB/c-*Kit*$^{+/+}$ PBS mice. For OVA-specific antibody levels, $n = 8$ for BALB/c-*Kit*$^{W\text{-}sh/W\text{-}sh}$ OVA, $n = 4$ for BALB/c-*Kit*$^{+/+}$ OVA, $n = 4$ for BALB/c-*Kit*$^{W\text{-}sh/W\text{-}sh}$ PBS, and $n = 3$ for BALB/c-*Kit*$^{+/+}$ PBS. **a**, **b**, **f**, **g** Data were pooled from age-matched mice from three separate experiments, each of which gave similar results. Mean values are shown ±s.e.m. (**a**) or + s.e.m. (**b**, **d**, **f**, **g**). Similar results were obtained from a second group of age-matched older mice. For Penh measurements, $^{**}p < 0.01$ for BALB/c-*Kit*$^{+/+}$ OVA vs. BALB/c-*Kit*$^{+/+}$ PBS, $^{*}p < 0.02$ for BALB/c-*Kit*$^{W\text{-}sh/W\text{-}sh}$ OVA vs. BALB/c-*Kit*$^{W\text{-}sh/W\text{-}sh}$ PBS as determined by 2-way ANOVA. For BALF cell counts and infiltrating leukocytes counts on histology, p values for t tests comparing BALB/c-*Kit*$^{+/+}$ PBS vs. BALB/c-*Kit*$^{+/+}$ OVA, BALB/c-*Kit*$^{W\text{-}sh/W\text{-}sh}$ PBS vs. BALB/c-*Kit*$^{W\text{-}sh/W\text{-}sh}$ OVA, and BALB/c-*Kit*$^{+/+}$ OVA vs. BALB/c-*Kit*$^{W\text{-}sh/W\text{-}sh}$ OVA that remained significant after correction for performing multiple t tests are shown (see Methods). For goblet cells counts, group means were compared by ANOVA. Mean antibody titers were compared by ANOVA.

Discussion

BALB/c-*Kit*$^{W\text{-}sh/W\text{-}sh}$ mice exhibited many of the features of their C57BL/6 counterparts. They exhibited a profound MC deficiency in most of the tissues examined (Fig. 1 and Table 1), with trace residual numbers of MCs in the skin of adult mice as was previously observed in C57BL/6-*Kit*$^{W\text{-}sh/W\text{-}sh}$ mice [4, 35]. However, we also observed trace numbers of MCs in lung and trachea of BALB/c-*Kit*$^{W\text{-}sh/W\text{-}sh}$ mice (Table 1) that were not seen in C57BL/6-*Kit*$^{W\text{-}sh/W\text{-}sh}$ mice [4]. Subtle differences from the corresponding wild type mice in hematologic profiles were observed in BALB/c-*Kit*$^{W\text{-}sh/W\text{-}sh}$ mice (Fig. 2), similar to those previously described in C57BL/6-*Kit*$^{W\text{-}sh/W\text{-}sh}$ mice [2, 4, 13, 16, 19]. The splenomegaly and increased splenic hematopoiesis (Fig. 2) we observed in our BALB/c-*Kit*$^{W\text{-}sh/W\text{-}sh}$ mice are consistent with previous observations in other BALB/c-*Kit*$^{W\text{-}sh/W\text{-}sh}$ and C57BL/6-*Kit*$^{W\text{-}sh/W\text{-}sh}$ mice [16, 36].

We examined three models of allergic inflammation in BALB/c-*Kit*$^{W\text{-}sh/W\text{-}sh}$ mice that were deficient in MCs. The first model, IgE-dependent passive cutaneous anaphylaxis, is a passive model of acute allergic inflammation that has previously been shown to be entirely MC-dependent in several different mouse strains, on several different genetic backgrounds [2, 24, 32, 37–39]. We similarly observed that IgE-dependent passive cutaneous anaphylaxis was undetectable in BALB/c-*Kit*$^{W\text{-}sh/W\text{-}sh}$ mice (Fig. 3), consistent with the inflammation in this model being largely or entirely MC-dependent, and indicating that genetic background may have little influence on this model of IgE-dependent acute allergic inflammation.

In contrast, we examined two active models of chronic allergic inflammation of the airways in which many immune and nonimmune cell types are thought to participate [27]. Prior work in MC-deficient mice with mutations affecting c-*kit* structure or expression indicated that many features of the OVA model in the C57BL/6 and WBB6F$_1$ backgrounds are substantially enhanced by MCs, including airway hyperresponsiveness to antigen, chronic inflammation of the airways, and airway goblet cell hyperplasia [27]. However, all three of these features developed in OVA-sensitized and challenged BALB/c-*Kit*$^{W\text{-}sh/W\text{-}sh}$ mice which had profoundly diminished numbers of tissue MCs (Fig. 4). Similarly, airway hyperresponsiveness and inflammation were at least partially diminished in MC-deficient C57BL/6-*Kit*$^{W\text{-}sh/W\text{-}sh}$ but not in MC-deficient BALB/c-*Kit*$^{W\text{-}sh/W\text{-}sh}$ mice in our new HDM model (Supplementary Fig. 2 and Fig. 5). Accordingly, these finding indicate that genetic background can strongly influence the importance of the contributions of MCs to the development of features of chronic allergic inflammation in these two models.

It is possible that other models of airway inflammation, using other antigens, sensitization schemes, or different amounts of antigen, may detect roles for MCs that are not as strongly influenced by genetic background as in those used in the present study. However, it is noteworthy that roles for MCs that were dependent on genetic background were similarly shown in both a different model of allergic airway inflammation and in a model of parasitic infection [24, 25]. Our observations, along with those from previously published models, support the conclusion that the importance of roles for MCs in models of allergic inflammation may be strongly influenced by genetic background.

Several possibilities may explain the differences we observed in the relative importance of genetic background in a model of IgE-dependent acute allergic inflammation vs. models for chronic allergic inflammation. First, as mentioned above, IgE-dependent passive cutaneous anaphylaxis elicited in naïve mice appears to be entirely MC-dependent whereas chronic allergic inflammation is a complex process involving multiple immune and nonimmune cell types and multiple inflammatory pathways. Therefore, MCs may have roles that are redundant or overlapping with other cell types in some models of chronic allergic inflammation. For

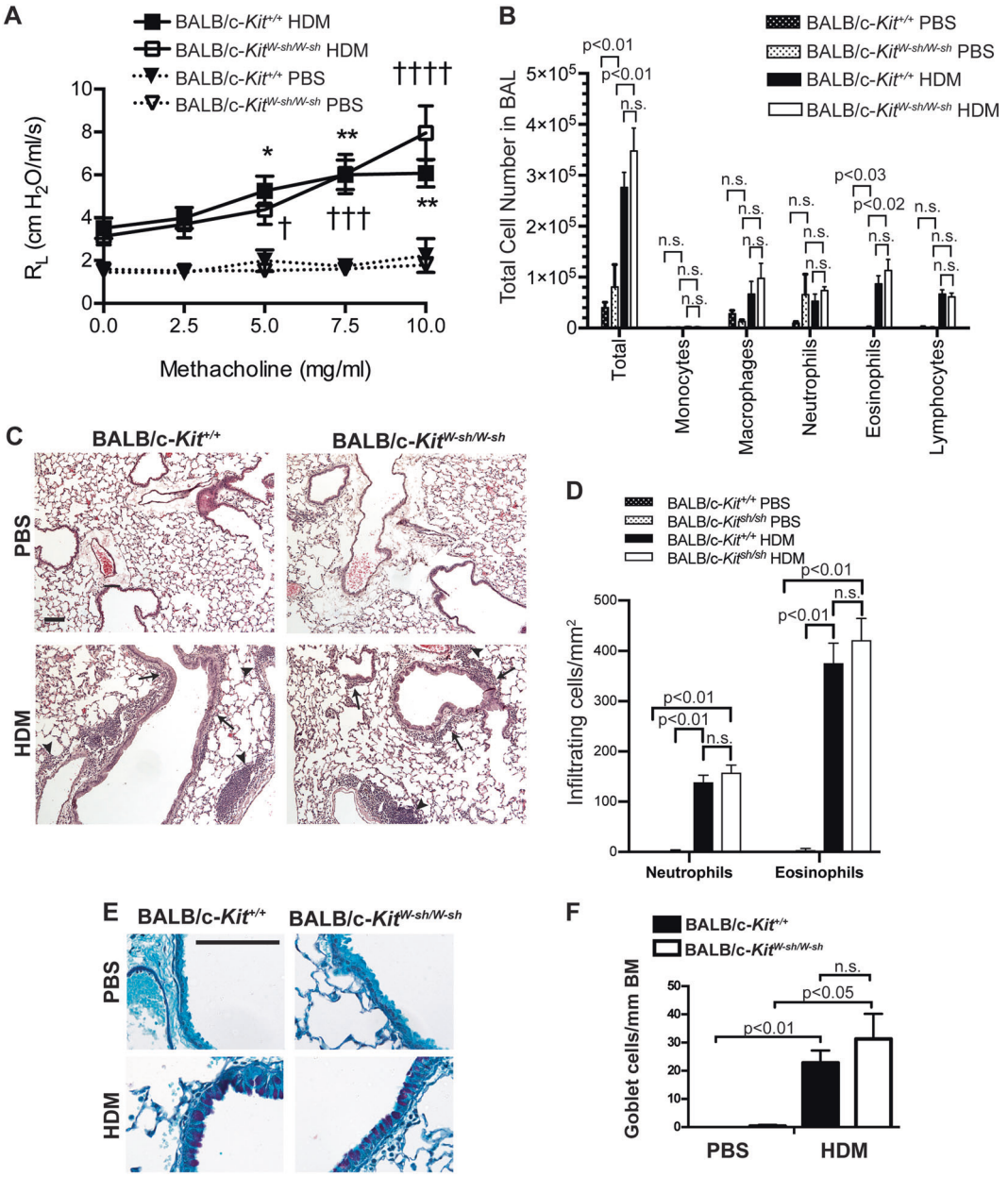

Fig. 5 Airway hyperresponsiveness to methacholine and lung inflammation develop in a house dust mite (HDM) model of chronic asthma elicited in BALB/c-*Kit*$^{W\text{-}sh/W\text{-}sh}$ mice. a Airway resistance (R_L) after aerosolized methacholine and lung inflammation were measured 1 day after the ninth intranasal challenge with HDM or PBS. **b** Leukocyte numbers in bronchoalveolar lavage fluid (BALF) obtained following airway measurements were determined by manual counting and by differential counts on cytospin slides. Histology in **c** H&E and **e** PAS-stained sections of lungs. In **c** solid arrowheads indicate perivascular inflammation and solid arrows indicate peribronchiolar inflammation. **d** Numbers of infiltrating leukocytes quantified per mm^2 of airway. **f** Goblet cell numbers per mm of airway basement membrane (BM) were measured in histological sections stained with PAS. Scale bars (**c**, **e**) indicate 100 µm. $n = 7$ for BALB/c-*Kit*$^{W\text{-}sh/W\text{-}sh}$ HDM, $n = 7$ for BALB/c-*Kit*$^{+/+}$ HDM, $n = 4$ for BALB/c-*Kit*$^{W\text{-}sh/W\text{-}sh}$ PBS, and $n = 3$ for BALB/c-*Kit*$^{+/+}$ PBS. Mean values ± s.e.m. (**a**) or + s.e.m. (**b**) are shown. For R_L measurements, $^{*}p < 0.05$, $^{**}p < 0.01$ for BALB/c-*Kit*$^{+/+}$ HDM vs. BALB/c-*Kit*$^{+/+}$ PBS, $^{\dagger}p < 0.05$, $^{\dagger\dagger\dagger}p < 0.001$, $^{\dagger\dagger\dagger\dagger}p < 0.0001$ for BALB/c-*Kit*$^{W\text{-}sh/W\text{-}sh}$ HDM vs. BALB/c-*Kit*$^{W\text{-}sh/W\text{-}sh}$ PBS, as determined by 2-way ANOVA. For BALF cell counts and infiltrating leukocytes counts on histology, p values for t tests comparing BALB/c-*Kit*$^{+/+}$ PBS vs. BALB/c-*Kit*$^{+/+}$ HDM, BALB/c-*Kit*$^{W\text{-}sh/W\text{-}sh}$ PBS vs. BALB/c-*Kit*$^{W\text{-}sh/W\text{-}sh}$ HDM, and BALB/c-*Kit*$^{+/+}$ OVA vs. BALB/c-*Kit*$^{W\text{-}sh/W\text{-}sh}$ HDM that remained significant after correction for performing multiple t tests are shown (see Methods). For goblet cells counts, group means were compared by ANOVA.

example, IL-4, IL-13, and IL-17A, produced by T cells, can enhance smooth muscle contraction in vitro and increase airway hyperresponsiveness induced by muscarinic agonists [40–42], and possibly antigens. This may be particularly relevant in BALB/c mice, as BALB/c mice have a general T_H2 bias with high levels of IgE production [23, 43].

Therefore, in some models of allergic airway inflammation, BALB/c mice may produce higher levels of cytokines that can influence airway function.

Second, a role for MCs may only be evident in models of allergic inflammation of the airways that are induced with relatively low levels of antigen exposure, as has previously been suggested in other models of airway hyperreactivity and cutaneous hypersensitivity [44, 45]. Third, there are small numbers of residual MCs that were observed in BALB/c-*Kit*$^{W\text{-}sh/W\text{-}sh}$ mice (Table 1) that were not observed in C57BL/6-*Kit*$^{W\text{-}sh/W\text{-}sh}$ mice [4]. However, it is difficult to hypothesize a role for these MCs in the inflammatory phenotype that would not be affected by their dramatically reduced numbers. Finally, Kit deficiency has been described to have certain MC-independent effects, such as a reduction of airway hyperresponsivness [9] and increased numbers of myeloid "suppressor" cells capable of blunting T cell responsiveness [36]. While we would expect each of these Kit phenotypes to blunt rather than enhance airway hyperresponsiveness and lung inflammation in BALB/c-*Kit*$^{W\text{-}sh/W\text{-}sh}$ mice, we cannot rule out the possibility that other MC-independent Kit effects may be more strongly expressed in the BALB/c than in the C57BL/6 background.

The choice of MC-deficient mouse models to study the roles of MCs in inflammation and other biologic processes requires consideration of multiple factors. Kit-deficient animals have multiple non-MC phenotypes [2, 4–16, 19] that may complicate the interpretation of any results obtained. For this reason, non-Kit dependent MC-deficient models can be advantageous, and both inducible [39, 46] and constitutive [37, 38, 46] non-Kit dependent MC-deficient models are now available. However, these models also have their limitations. Some of the genetic approaches used to create such mice can have effects on other immune cells, such as T cells and granulocytes (including basophils) [37, 38], and depletion of cells with diphtheria toxin may also have effects on cells not expressing the receptor. While these issues are not yet as well understood as are some of the shortcomings of the Kit-deficient models, they should be kept in mind. Our results indicate that, when choosing a MC-deficient model, particularly for chronic inflammatory conditions, one also will need to consider the possible effects of genetic background on the importance of the MC's potential roles in that model.

In conclusion, the new strain of BALB/c-*Kit*$^{W\text{-}sh/W\text{-}sh}$ mice described herein permits addition of results from another mouse model of MC deficiency in studies of the potential roles of MCs in inflammation and other biological responses. Having a larger number of available MC-deficient mouse models will help to define the roles of MCs in inflammatory processes and other biologic responses, and also will help in efforts to identify which of these roles may be more or less dependent on the genetic background of the mouse strains tested.

Acknowledgements We thank Mariola Liebersbach and Chen Liu for technical assistance with mouse breeding and histology. Support: This work was supported by National Institute of Health Grants CA72074, AI070813, AI23990 and AR067145 to SJG and by the Department of Pathology of Stanford University School of Medicine. JDH and RS were supported by fellowships/grants from the Lucile Packard Foundation for Children's Health and Stanford CTSA (UL1 RR025744 & TR001085). JDH also was supported by a diversity supplement to AI104209 (to SJG), NIH T32 AI07290, The Tashia and John Morgridge Endowed Postdoctoral Fellowship, AAAAI Mylan Anaphylaxis Award and The Sean N. Parker Center for Allergy & Asthma Research.

Compliance with ethical standards

Conflict of interest The authors declare that they have no conflict of interest.

Publisher's note Springer Nature remains neutral with regard to jurisdictional claims in published maps and institutional affiliations.

References

1. Galli SJ, Tsai M, Marichal T, et al. Approaches for analyzing the roles of mast cells and their proteases in vivo. Adv Immunol. 2015;126:45–127.
2. Reber LL, Marichal T, Galli SJ. New models for analyzing mast cell functions in vivo. Trends Immunol. 2012;33:613–25.
3. Rodewald HR, Feyerabend TB. Widespread immunological functions of mast cells: fact or fiction? Immunity. 2012;37:13–24.
4. Grimbaldeston MA, Chen CC, Piliponsky AM, et al. Mast cell-deficient W-sash c-kit mutant Kit W-sh/W-sh mice as a model for investigating mast cell biology in vivo. Am J Pathol. 2005; 167:835–48.
5. Kitamura Y, Go S, Hatanaka K. Decrease of mast cells in W/Wv mice and their increase by bone marrow transplantation. Blood. 1978;52:447–52.
6. Nakano T, Sonoda T, Hayashi C, et al. Fate of bone marrow-derived cultured mast cells after intracutaneous, intraperitoneal, and intravenous transfer into genetically mast cell-deficient W/Wv mice. Evidence that cultured mast cells can give rise to both connective tissue type and mucosal mast cells. J Exp Med. 1985; 162:1025–43.
7. Tsai M, Grimbaldeston MA, Yu M, et al. Using mast cell knock-in mice to analyze the roles of mast cells in allergic responses in vivo. Chem Immunol Allergy. 2005;87:179–97.
8. Mallen-St Clair J, Pham CT, Villalta SA, et al. Mast cell dipeptidyl peptidase I mediates survival from sepsis. J Clin Investig. 2004;113:628–34.
9. Cozzi E, Ackerman KG, Lundequist A, et al. The naive airway hyperresponsiveness of the A/J mouse is Kit-mediated. Proc Natl Acad Sci USA. 2011;108:12787–92.
10. Galli SJ, Arizono N, Murakami T, et al. Development of large numbers of mast cells at sites of idiopathic chronic dermatitis in genetically mast cell-deficient WBB6F1-W/Wv mice. Blood. 1987;69:1661–6.
11. Kitamura Y, Yokoyama M, Matsuda H, et al. Coincidental development of forestomach papilloma and prepyloric ulcer in nontreated mutant mice of W/Wv and Sl/Sld genotypes. Cancer Res. 1980;40:3392–7.

12. Nakano T, Waki N, Asai H, et al. Different repopulation profile between erythroid and nonerythroid progenitor cells in genetically anemic W/Wv mice after bone marrow transplantation. Blood. 1989;74:1552–6.
13. Piliponsky AM, Chen CC, Grimbaldeston MA, et al. Mast cell-derived TNF can exacerbate mortality during severe bacterial infections in C57BL/6-KitW-sh/W-sh mice. Am J Pathol. 2010; 176:926–38.
14. Shimada M, Kitamura Y, Yokoyama M, et al. Spontaneous stomach ulcer in genetically mast-cell depleted W/Wv mice. Nature. 1980;283:662–4.
15. Puddington L, Olson S, Lefrancois L. Interactions between stem cell factor and c-Kit are required for intestinal immune system homeostasis. Immunity. 1994;1:733–9.
16. Nigrovic PA, Gray DH, Jones T, et al. Genetic inversion in mast cell-deficient (Wsh) mice interrupts corin and manifests as hematopoietic and cardiac aberrancy. Am J Pathol. 2008;173:1693–701.
17. Duttlinger R, Manova K, Berrozpe G, et al. The Wsh and Ph mutations affect the c-kit expression profile: c-kit misexpression in embryogenesis impairs melanogenesis in Wsh and Ph mutant mice. Proc Natl Acad Sci USA. 1995;92:3754–8.
18. Nagle DL, Kozak CA, Mano H, et al. Physical mapping of the Tec and Gabrb1 loci reveals that the Wsh mutation on mouse chromosome 5 is associated with an inversion. Hum Mol Genet. 1995;4:2073–9.
19. Zhou JS, Xing W, Friend DS, et al. Mast cell deficiency in Kit(W-sh) mice does not impair antibody-mediated arthritis. J Exp Med. 2007;204:2797–802.
20. Kim HY, DeKruyff RH, Umetsu DT. The many paths to asthma: phenotype shaped by innate and adaptive immunity. Nat Immunol. 2010;11:577–84.
21. Laprise C, Bouzigon E. The genetics of asthma and allergic diseases: pieces of the puzzle are starting to come together. Curr Opin Allergy Clin Immunol. 2013;13:461–2.
22. von Mutius E. Gene-environment interactions in asthma. J Allergy Clin Immunol. 2009;123:3–11.
23. Boyce JA, Austen KF. No audible wheezing: nuggets and conundrums from mouse asthma models. J Exp Med. 2005; 201:1869–73.
24. Becker M, Reuter S, Friedrich P, et al. Genetic variation determines mast cell functions in experimental asthma. J Immunol. 2011;186:7225–31.
25. Blankenhaus B, Reitz M, Brenz Y, et al. Foxp3(+) regulatory T cells delay expulsion of intestinal nematodes by suppression of IL-9-driven mast cell activation in BALB/c but not in C57BL/6 mice. PLoS Pathog. 2014;10:e1003913.
26. Yu M, Eckart MR, Morgan AA, et al. Identification of an IFN-gamma/mast cell axis in a mouse model of chronic asthma. J Clin Investig. 2011;121:3133–43.
27. Yu M, Tsai M, Tam SY, et al. Mast cells can promote the development of multiple features of chronic asthma in mice. J Clin Investig. 2006;116:1633–41.
28. Liu FT, Bohn JW, Ferry EL, et al. Monoclonal dinitrophenyl-specific murine IgE antibody: preparation, isolation, and characterization. J Immunol. 1980;124:2728–37.
29. Sibilano R, Gaudenzio N, DeGorter MK, et al. A TNFRSF14-FcεRI-mast cell pathway contributes to development of multiple features of asthma pathology in mice. Nat Commun. 2016;7:13696.
30. Starkl P, Marichal T, Gaudenzio N, et al. IgE antibodies, FcεRIα, and IgE-mediated local anaphylaxis can limit snake venom toxicity. J Allergy Clin Immunol. 2015;137:246–57.
31. The Jackson Laboratory, Reproductive performance survey, females of 33 inbred strains of mice. Mouse Phenome Database web site, MPD:14943, The Jackson Laboratory, Bar Harbor, Maine. http://phenome.jax.org. Accessed 9 April 2015.
32. Wershil BK, Mekori YA, Murakami T, et al. 125I-fibrin deposition in IgE-dependent immediate hypersensitivity reactions in mouse skin. Demonstration of the role of mast cells using genetically mast cell-deficient mice locally reconstituted with cultured mast cells. J Immunol. 1987;139:2605–14.
33. Calderon MA, Linneberg A, Kleine-Tebbe J, et al. Respiratory allergy caused by house dust mites: What do we really know? J Allergy Clin Immunol. 2015;136:38–48.
34. Schulze J, Reinmuller W, Herrmann E, et al. Bronchial allergen challenges in children—safety and predictors. Pediatr Allergy Immunol. 2013;24:19–27.
35. Yamazaki M, Tsujimura T, Morii E, et al. C-kit gene is expressed by skin mast cells in embryos but not in puppies of Wsh/Wsh mice: age-dependent abolishment of c-kit gene expression. Blood. 1994;83:3509–16.
36. Michel A, Schuler A, Friedrich P, et al. Mast cell-deficient Kit(W-sh) "Sash" mutant mice display aberrant myelopoiesis leading to the accumulation of splenocytes that act as myeloid-derived suppressor cells. J Immunol. 2013;190:5534–44.
37. Feyerabend TB, Weiser A, Tietz A, et al. Cre-mediated cell ablation contests mast cell contribution in models of antibody- and T cell-mediated autoimmunity. Immunity. 2011;35:832–44.
38. Lilla JN, Chen CC, Mukai K, et al. Reduced mast cell and basophil numbers and function in Cpa3-Cre; Mcl-1fl/fl mice. Blood. 2011;118:6930–8.
39. Sawaguchi M, Tanaka S, Nakatani Y, et al. Role of mast cells and basophils in IgE responses and in allergic airway hyperresponsiveness. J Immunol. 2012;188:1809–18.
40. Grunstein MM, Hakonarson H, Leiter J, et al. IL-13-dependent autocrine signaling mediates altered responsiveness of IgE-sensitized airway smooth muscle. Am J Physiol Lung Cell Mol Physiol. 2002;282:L520–8.
41. Kudo M, Melton AC, Chen C, et al. IL-17A produced by alpha-beta T cells drives airway hyper-responsiveness in mice and enhances mouse and human airway smooth muscle contraction. Nat Med. 2012;18:547–54.
42. Perkins C, Yanase N, Smulian G, et al. Selective stimulation of IL-4 receptor on smooth muscle induces airway hyperresponsiveness in mice. J Exp Med. 2011;208:853–67.
43. Brewer JP, Kisselgof AB, Martin TR. Genetic variability in pulmonary physiological, cellular, and antibody responses to antigen in mice. Am J Respir Crit Care Med. 1999;160:1150–6.
44. Kobayashi T, Miura T, Haba T, et al. An essential role of mast cells in the development of airway hyperresponsiveness in a murine asthma model. J Immunol. 2000;164:3855–61.
45. Norman MU, Hwang J, Hulliger S, et al. Mast cells regulate the magnitude and the cytokine microenvironment of the contact hypersensitivity response. Am J Pathol. 2008;172:1638–49.
46. Dudeck A, Dudeck J, Scholten J, et al. Mast cells are key promoters of contact allergy that mediate the adjuvant effects of haptens. Immunity. 2011;34:973–84.

Titles and legends to supplemental figures

Supplemental Figure 1. Lung cytokines and chemokines in an OVA-elicited model of chronic asthma in BALB/c-*Kit*$^{W\text{-}sh/W\text{-}sh}$ mice. Concentrations of IL-5, RANTES (CCL5) and eotaxin-1 (CCL11) were measured in lung homogenates. In OVA sensitized and challenged groups, N=9 for BALB/c-*Kit*$^{W\text{-}sh/W\text{-}sh}$ and N=5 for BALB/c-*Kit*$^{+/+}$ mice; in PBS mock-sensitized and challenged groups, N=4 for BALB/c-*Kit*$^{W\text{-}sh/W\text{-}sh}$ and N=3 for BALB/c-*Kit*$^{+/+}$ mice. Lines represent mean values ± s.e.m. Values were compared by ANOVA.

Supplemental Figure 2. Airway hyperresponsiveness to methacholine and lung inflammation develop in a house dust mite (HDM) mouse model of chronic asthma elicited in C57BL/6-*Kit*$^{W\text{-}sh/W\text{-}sh}$ mice. **A.** Airway resistance (R_L) in response to aerosolized methacholine was measured 1 day after the ninth intranasal challenge with HDM or PBS. **B.** Leukocyte numbers in bronchoalveolar lavage fluid (BALF) obtained after airway measurements were determined by manual counting and microscopic differential. Histology in (**C**) H&E and (**E**) PAS-stained sections of lungs. In (**C**) solid arrowheads indicate perivascular inflammation and solid arrows indicate peribronchiolar inflammation. **D.** Numbers of infiltrating leukocytes quantified per mm^2 of airway. **F**. Goblet cell numbers per mm of airway basement membrane (BM) were measured in histological sections stained with PAS. Scale bars (**C** & **E**) indicate 100 μm. In HDM sensitized and challenged groups, N=7 for C57BL/6-*Kit*$^{W\text{-}sh/W\text{-}sh}$ and N=6 for C57BL/6-*Kit*$^{+/+}$ mice; in PBS mock-sensitized and challenged groups, N=3 for C57BL/6-*Kit*$^{W\text{-}sh/W\text{-}sh}$

and N=3 for C57BL/6-*Kit*$^{+/+}$ PBS. Mean values ± s.e.m. (**A**) or + s.e.m. (**B**) are shown. For R_L measurements, * p<0.05, **p<0.01 for C57BL/6-*Kit*$^{+/+}$ HDM vs C57BL/6-*Kit*$^{+/+}$ PBS, † p<0.05, ††† P<0.001, †††† p<0.0001 for C57BL/6-*Kit*$^{W\text{-}sh/W\text{-}sh}$ HDM vs. C57BL/6-*Kit*$^{W\text{-}sh/W\text{-}sh}$ PBS as determined by 2-way ANOVA. For BALF cell counts and infiltrating leukocyte counts on histology, p values for *t* tests comparing C57BL/6-*Kit*$^{+/+}$ PBS vs C57BL/6-*Kit*$^{+/+}$ HDM, C57BL/6-*Kit*$^{W\text{-}sh/W\text{-}sh}$ PBS vs. C57BL/6-*Kit*$^{W\text{-}sh/W\text{-}sh}$ HDM, and C57BL/6-*Kit*$^{+/+}$ HDM vs C57BL/6-*Kit*$^{W\text{-}sh/W\text{-}sh}$ HDM that remained significant after correction for performing multiple *t* tests are shown (see Methods). For goblet cell counts, group means were compared by ANOVA.

Suppl. Figure 1

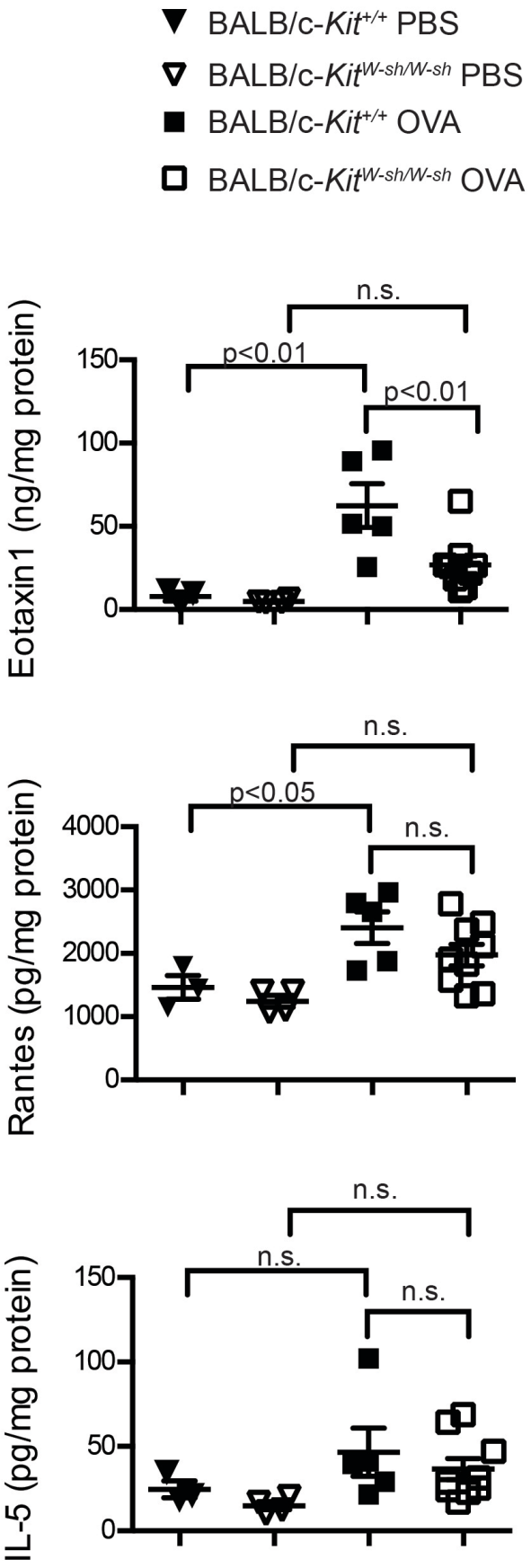
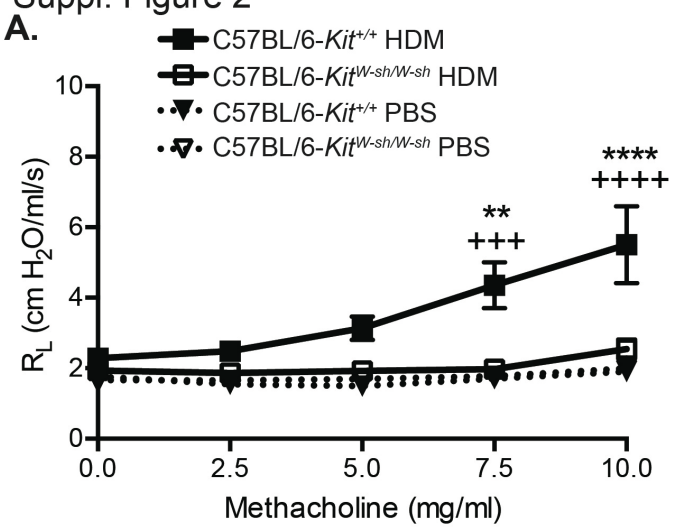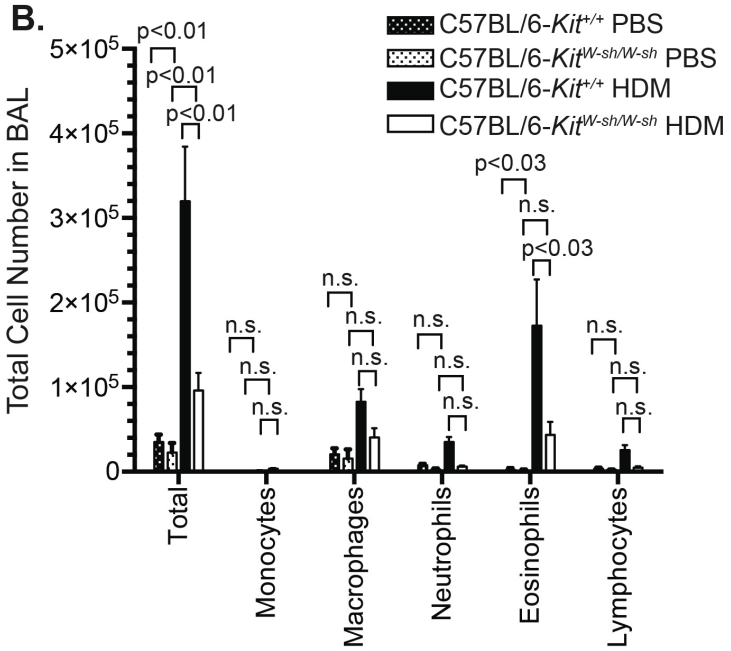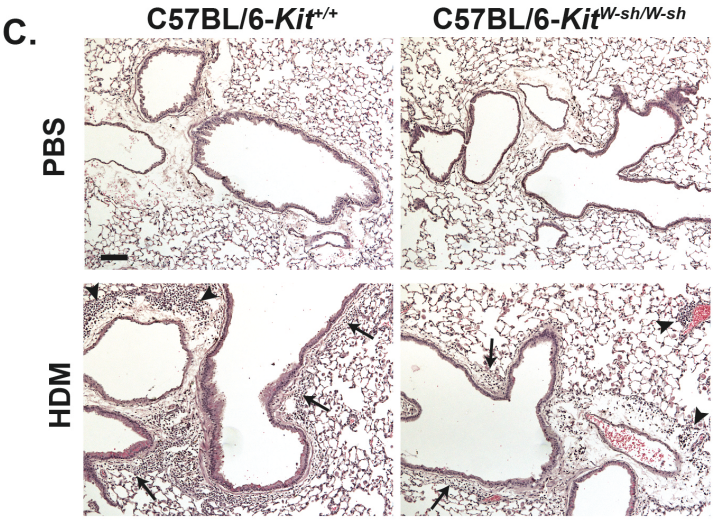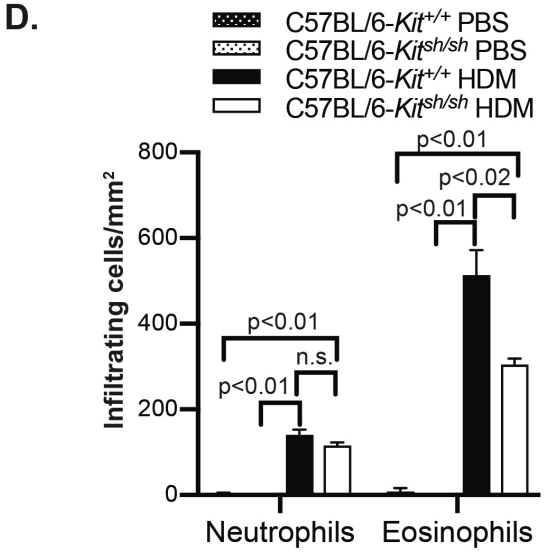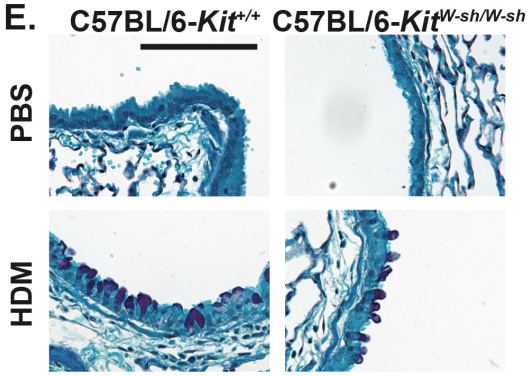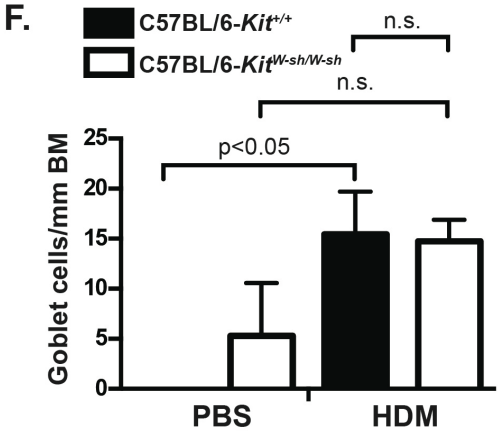
Suppl. Figure 2